Investigation of a dye ring laser with backscattering

F. C. Cheng
Department of Physics and Astronomy, University of Rochester, Rochester, New York 14627
(Received 4 November 1991)

The dynamics of the two counterpropagating modes of a dye ring laser with backscattering have been studied experimentally. By varying the power of the pump laser, we have observed the dye-laser intensities change from random switching to anticorrelated oscillations. When the magnitude of the backscattering coefficient R is close to the critical value R_c, the laser exhibits noise-induced transition between the switching region and the oscillation region. This noise-induced effect can be attributed to pump fluctuations. A frequency lock-in effect has been observed in the oscillation region when $|R|$ is near R_c. The experimental results are compared with solutions obtained both from the analysis of the third-order equations of motion and from the Monte Carlo simulations of these equations with additive and multiplicative noise.

PACS number(s): 42.60.−v, 05.40.+j

I. INTRODUCTION

The effects of backscattering in ring lasers have attracted a great deal of interest since the application of a He-Ne ring laser as a gyroscope [1]. Backscattering causes frequency lock-in between the two counterpropagating modes when the laser is used as a gyroscope. Even for a nonrotating ring laser, backscattering can have a major effect on the behavior of the two modes [2–16]. Studies of the inhomogeneously broadened ring laser have shown that under certain conditions the two counterpropagating modes can exhibit anticorrelated oscillations [2–8] and sudden π changes of their phase difference [4,5,7]. Both anticorrelated oscillations and sudden π changes of the phase difference have been observed experimentally in a He-Ne ring laser [4,5,8].

In a homogeneously broadened ring laser, on the other hand, the two counterpropagating modes exhibit random intensity switching when the laser is operated above threshold [17–20]. In this case backscattering can drastically change the behavior of the laser and suppress the mode switching [2,3,12–16]. Kuhlke and Jetschke [2] first showed the existence of a critical value R_c of the backscattering coefficient R for instabilities to develop in a homogeneously broadened laser, by analyzing the deterministic equations of motion without noise terms. For the case of $|R|$ less than R_c, they obtained a stable solution for the two mode intensities when the backscattering is "off phase." Their results do not show the usual random switching of the intensities because of the absence of additive noise terms in the equations. When $|R|$ is larger than R_c, they obtained solutions of self-sustained intensity oscillations. Their solutions showed that the oscillations are anharmonic when $|R|$ is close to R_c and become harmonic in the limit of large $|R|$. These intensity oscillations have been observed experimentally in ring dye lasers [14,15]. Recently, we have used Monte Carlo simulations to study the equations of motion with backscattering and in the presence of both additive noise and multiplicative noise [16]. Our simulation results indicate that the laser with "off phase" backscattering has two regions of operation: the switching region and the oscillation region. The model also shows that a sudden change of phase difference of π between the two modes can occur in both regions whenever one of the two intensities is zero. The most interesting feature to emerge from the simulations is the multiplicative-noise-driven transition from one region to another when $|R|$ is close to R_c.

Recently, Spreeuw *et al.* [8], using a standing-wave representation for the coupled equations of motion instead of the usual traveling-wave representation, interpreted the intensity oscillations to result from the frequency splitting of the mode structure of the corresponding passive ring cavity. They experimentally observed the frequency splitting in a He-Ne laser [8] and in a ring dye laser [15]. Using their standing-wave approach, they also showed theoretically the existence of R_c in a homogeneously broadened ring laser.

In this paper we report on experiments performed on a dye ring laser with backscattering. The two mode intensities of the laser in both the switching and the oscillation regions have been measured. When $|R|$ is close to R_c, we observe noise-induced transitions between the switching region and the oscillation region. The experimental results are compared with our previous conclusions from computer simulations [16]. We also observe a frequency lock-in effect in the oscillation region. For a laser gyroscope, the frequency splitting is associated with the rotation rate of the gyroscope, and the lock-in effect is due to the backscattering. In our case, the frequency splitting is connected with the backscattering and the lock-in effect is due to cross saturation of the two counterpropagating modes. We also observe frequency splitting in our measurements. The experimental results are compared with the solution of the deterministic equations and with the results from the Monte Carlo simulations.

II. EQUATIONS OF MOTION

The starting point for our treatment is the semiclassical third-order coupled equations of motion for two modes of a single-frequency homogeneously broadened ring laser. With the introduction of additional terms representing backscattering, additive noise, and multiplicative noise, the equations of motion can be written in the following dimensionless form [10,20]:

$$\dot{E}_1=(a_1-|E_1|^2-2|E_2|^2)E_1+R_1E_2+pE_1+q_1 ,$$
$$\dot{E}_2=(a_2-|E_2|^2-2|E_1|^2)E_2+R_2E_1+pE_2+q_2 , \quad (1)$$

$$\langle q_i^*(t)q_j(t')\rangle=4\delta_{ij}\delta(t-t') \quad (i,j=1,2) , \quad (2)$$

$$\langle p^*(t)p(t')\rangle=\frac{Q}{T_p}\exp\left[-\frac{|t-t'|}{T_p}\right] , \quad (3)$$

$$R_j=|R_j|e^{i\theta_j}, \quad E_j=|E_j|e^{i\phi_j} \quad (j=1,2) , \quad (4)$$

$$\phi(t)=\phi_2-\phi_1 , \quad (5)$$

$$\delta\theta=\pi-(\theta_1+\theta_2) . \quad (6)$$

Here E_1 and E_2 are the complex dimensionless amplitudes of the two counter-propagating modes, a_1 and a_2 are their corresponding real pump parameters, R_1 and R_2 are the dimensionless complex backscattering coefficients, $q_1(t)$ and $q_2(t)$ are δ-correlated noise terms representing spontaneous emission fluctuations and other additive noise, $p(t)$ is the colored multiplicative noise representing the pump fluctuations, Q is the strength of the pump noise, and T_p is the correlation time associated with the pump fluctuations. The backscattering is customarily said to be "off phase" when $\theta_1+\theta_2=(2n+1)\pi$ and "in phase" when $\theta_1+\theta_2=2n\pi$ (n is an integer) [2]. We include multiplicative-noise terms in our equations because the effects of pump fluctuations are known to be significant for a dye laser operated not far above threshold [20–22,26]. The multiplicative noise is also important in explaining the dynamics of the laser when $|R|$ is close to R_c. Since there is no simple analytic solution for these nonlinear stochastic equations, numerical solutions are obtained by using Monte Carlo simulations in Sec. III.

If the multiplicative-noise terms are neglected, the steady-state solution for Eq. (1) can be obtained analytically under certain conditions. To the coupled Eq. (1) without multiplicative-noise terms, there corresponds a four-dimensional Fokker-Planck equation for the joint probability density $P(E_1,E_2,t)$. The steady-state solution $P_s(E_1,E_2)$ for the joint probability density when $R_1=R_2^*$, is given by

$$P_s(E_1,E_2)=\text{const}\times\exp\{\tfrac{1}{2}a_1|E_1|^2+\tfrac{1}{2}a_2|E_2|^2-\tfrac{1}{4}|E_1|^4-\tfrac{1}{4}|E_2|^4-|E_1|^2|E_2|^2+[\tfrac{1}{4}(R_1+R_2^*)E_1^*E_2+\text{c.c.}]\} . \quad (7)$$

After integrating over the phase difference ϕ, we have for the joint probability density of the two mode intensities:

$$P(I_1,I_2)=\text{const}\times I_0(|R|\sqrt{I_1I_2})\times\exp[\tfrac{1}{2}(a_1I_1+a_2I_2)-\tfrac{1}{4}I_1^2-\tfrac{1}{4}I_2^2-I_1I_2] , \quad (8)$$

where $I_1=|E_1|^2$, $I_2=|E_2|^2$, $|R|=|R_1|=|R_2|$, and I_0 is the modified Bessel function of zero order. This steady-state solution for $R_1=R_2^*$ corresponds to the case of "in phase" backscattering. For other situations including the case of "off phase" backscattering, no steady-state solution has been obtained, because the potential conditions for the Fokker-Planck equations are not satisfied. Similar results have been obtained by Christian and Mandel [10] for an inhomogeneously broadened ring laser operating at line center with equal pump parameter.

When both additive noise and multiplicative noise are neglected, the deterministic equations for a homogeneously broadened ring laser have been studied by Kuhlke and Jetschle [2]. The solution for R_c for "off phase" backscattering with $|R_1|=|R_2|$ has been found to be

$$R_c=\frac{a(\xi-1)}{2\sqrt{2(\xi+1)}} , \quad (9)$$

where ξ is the cross coupling constant for the two modes and $a(=a_1=a_2)$ is the pump parameter. ξ is 2 for a homogeneously broadened laser and is 1 for an inhomogeneously broadened laser. For a dye ring laser, $\xi=2$ and $R_c=a/2\sqrt{6}$. The same expression for R_c has also been derived by using a standing-wave approach [15]. The ratio of the amplitudes of the two switching modes at the critical location where $|R|=R_c$ is given by [2]

$$\eta_{c1,c2}=[\xi+2\pm\sqrt{2(\xi+1)}]^{1/2} \quad (10)$$

and $\eta_{c1}=1/\eta_{c2}$. For $\xi=2$, η_{c1}^2 and η_{c2}^2 are, respectively, equal to 7.9 and 0.13.

III. MONTE CARLO SIMULATIONS

Numerical solutions of the coupled equations of motion [Eqs. (1)–(6)] have been obtained by using Monte Carlo simulations [16]. Figure 1 shows the computer results for the two mode intensities $I_1(t)$ and $I_2(t)$ as a function of time. The values of Q and T_p used in the simulations are, respectively, 100 and 0.5 based on previous measurements [21,22]. The pump parameter a is taken to be 100 and the corresponding R_c is calculated to be 20.4 from Eq. (9). The value of $|R|$ is 120 and is much larger than R_c, with $|R|/R_c=6.0$. The intensity oscillations are seen to be harmonic and anticorrelated. These results are consistent with those predicted from the deterministic analysis [2]. The period of the oscillations in dimensionless units is 0.027. This is close to the value 0.026 determined by using the formula $T=\pi/|R|$ [5]. In this simulation the value of $\delta\theta$ is 10°. Because $\delta\theta$ is not equal to zero, the modulation of the two intensity modu-

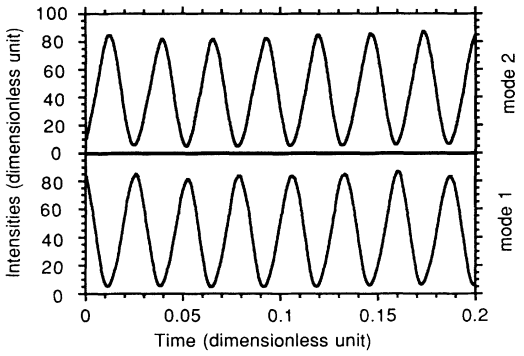

FIG. 1. Plots of dimensionless intensities vs dimensionless time from Monte Carlo simulations on Eqs. (1)–(6), with dimensionless iteration step size equal to 0.000 001, $a_1=a_2=a=100$, $|R_1|=|R_2|=|R|=120$, $\theta_1=\theta_2=85°$ ($\delta\theta=10°$), $Q=100$, and $T_p=0.5$. $R_c=20.4$ and $|R|/R_c=6$. The two intensities exhibit anticorrelated harmonic oscillations.

lations is not 100% and neither one of the two modes vanishes at any time. The computer solutions also indicate that sudden changes of π in the relative phase of the two modes do not occur under these conditions. The π-phase changes take place only when $\delta\theta$ is equal to or very close to zero and one of the two mode intensities vanishes. Simulation results also show that for fixed values of $|R|$ and a, although the intensity modulation decreases with increasing $\delta\theta$, the oscillation frequency remains the same and does not depend on the value of $\delta\theta$.

Figure 2 shows the time evolutions of the two mode intensities when $|R|$ is near but larger than R_c. The pump parameter used is 80 and $|R|$ is 20. From Eq. (9), R_c is calculated to be 16.3. Compared with the situation shown in Fig. 1, $|R|$ is closer to R_c this time. The ratio of $|R|/R_c=1.2$ and $\delta\theta=10°$. The intensity oscillations are anharmonic and have a period of 0.21. This value is quite different from the period 0.16 obtained from the formula $T=\pi/|R|$. This is due to an effect similar to the frequency lock-in effect in a ring-laser gyroscope, and will be discussed in more detail below. Small fluctuations in the intensity profiles and small variations in the periods of the individual oscillations are due to the multiplicative noise. Although the oscillating mode intensities appear to vanish at certain times, the corresponding computer results for the relative phase of the two modes do not show any sudden π-phase changes. If we compare Figs. 1 and 2, for the same values of $\delta\theta$, we see that the intensity modulation in Fig. 2, where $|R|=20$, is closer to 100% than that in Fig. 1, where $|R|=100$. Other simulations show that for a fixed and nonzero $\delta\theta$, the intensity modulation increases with decreasing $|R|$.

Figure 3 shows the two mode intensities as a function of time when $|R|$ is very close to R_c. The pump parameter used is 100, corresponding to $R_c=20.4$, and $|R|$ is 20. The two intensities now exhibit both random switching and anticorrelated oscillations. Similar results have been obtained previously by the author [16]. Figure 3 shows that there exists a certain threshold value of the intensities, above which the laser exhibits switching, whereas below it exhibits oscillation. This can be explained by taking account of the pump fluctuations. The effect of pump fluctuations on backscattering can be understood by replacing the constant pump parameter a by a random pump parameter,

$$A=a+p\ , \tag{11}$$

where $a\,(=a_1=a_2)$ is the constant pump parameter and p is the multiplicative-noise term. Equation (9) is then replaced by

$$R_c=\frac{\xi-1}{2\sqrt{2(\xi+1)}}A=\frac{\xi-1}{2\sqrt{2(\xi+1)}}(a+p)\ . \tag{12}$$

R_c can be interpreted as having a random component which is determined by the pump fluctuations. Whether the two modes exhibit random switching or periodic oscillations depends on whether $|R|$ is smaller or larger than R_c at that instant of time. This phenomenon can also be viewed as a consequence of the laser being in-

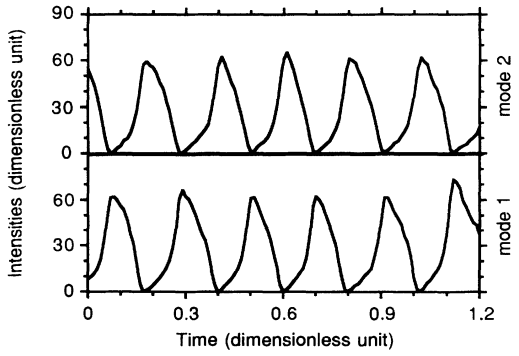

FIG. 2. Time evolution of intensities obtained from Monte Carlo simulations on Eqs. (1)–(6) with dimensionless iteration step size equal to 0.000 05, $a_1=a_2=a=80$, $|R_1|=|R_2|=|R|=20$, $\theta_1=\theta_2=85°$ ($\delta\theta=10°$), $Q=100$, and $T_p=0.5$. $R_c=16.3$ and $|R|/R_c=1.2$. The intensities exhibit anharmonic oscillations.

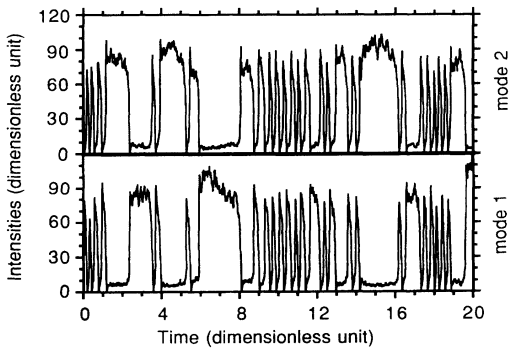

FIG. 3. Time evolution of the two intensities obtained from Monte Carlo simulations on Eqs. (1)–(6) with dimensionless iteration step size equal to 0.000 05, $a_1=a_2=a=100$, $|R_1|=|R_2|=|R|=20$, $\theta_1=\theta_2=85°$ ($\delta\theta=10°$), $Q=100$, and $T_p=0.5$. $|R|$ is near the critical value $R_c(=20.4)$.

directly driven by multiplicative noise to operate between the random-switching region and the periodic-oscillation region.

It is well known that a dye ring laser exhibits random mode switching when there is no backscattering. When one mode switches on, the other mode switches off and only one of the two counterpropagating modes is on at one time. The most probable intensity of the "off" mode is zero. But in the presence of backscattering, the most probable intensity of the "off" mode is no longer zero, although it is still small compared to the intensity of the "on" mode. This effect has been predicted from the deterministic analysis [2] and it can be seen in the switching region in Fig. 3. The ratio of the mean intensity of the "on" mode to the mean intensity of the "off" mode is estimated to be about 8 from Fig. 3, and this is consistent with the value of 7.9 obtained from the deterministic calculation at $|R|=R_c$. Our simulation results also show that the magnitude of the mean intensity of the "off" mode increases with increasing strength of backscattering, provided $|R|<R_c$, and the ratio of the mean intensity of the "on" mode to the mean intensity of the "off" mode increases with increasing a.

Figure 4 shows a plot of the frequency of the oscillations versus the magnitude of the backscattering coefficient. The dotted line represents $\omega/2=|R|$. The five solid curves are solutions for the cases $a=70$, 100, 150, 200, and 250 (from left to right). Each curve is obtained from Monte Carlo simulations based on the coupled equations of motion, Eqs. (1)–(6). The multiplicative-noise terms were neglected in these simulations and only the additive-noise terms were included. This is because including multiplicative-noise terms is equivalent to adding a stochastic component to the pump parameter. In order to obtain a well-defined value of the pump parameter, many realizations are required, and this was beyond the computational ability of our VAX station. However, the coupled equations indicate that the results without multiplicative noise should be similar to those with multiplicative noise. The graphs shown in Fig. 4 are similar to the frequency lock-in graphs obtained previously for a ring-laser gyroscope [1,23,24]. In the gyro case the lock-in effect is attributed to the backscattering and the beat frequency of the two counterpropagating modes is proportional to the rotation rate. In our case, the frequency of the oscillations is related to the magnitude of the backscattering coefficient while the lock-in effect is associated with the cross saturation of the two modes. The role of the cross saturation in the lock-in effect can be easily understood if the equation of motion for the phase difference is written in the standing-wave representation [15] and then compared with the phase equation for the laser gyroscope [23]. A similar phase equation has been obtained by Lamb to explain the frequency-locking phenomenon of a three-frequency laser [25].

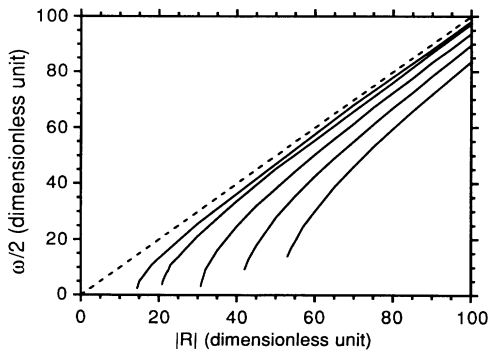

FIG. 4. Plots of intensity oscillation frequency vs $|R|$ obtained from Monte Carlo simulations. Both axes are in dimensionless units. The dotted line is $\omega/2=|R|$. The five solid curves are simulation results for $a=70$, 100, 150, 200, and 250 (from left to right). This diagram is similar to the frequency lock-in diagram for a ring-laser gyroscope.

When $|R|$ is close to R_c and in the absence of multiplicative noise, simulation results show that the additive noise is also involved in driving the laser between oscillation and switching regions. The effect of the additive noise is not significant in the previous simulations because the strength of the multiplicative noise has been assumed to be comparatively larger. Near the region $|R|=R_c$, we were not able to obtain a well-defined value of the oscillation frequency because the intensities become extremely anharmonic and it is hard to distinguish between oscillations and switchings. If one interprets the switching region as the one where the system is locked and the oscillation region as the one where the system is unlocked, then both additive and multiplicative noise could be described as being responsible for locking and unlocking the system. Centeno Neelen *et al.* [15] have numerically studied the deterministic equations of motion when $|R|>R_c$ and obtained a similar lock-in diagram. Because they have not included the effect of noise, their results showed a well-defined oscillation frequency even when $|R|$ is very close to R_c. Cresser *et al.* have studied the effect of quantum noise in He-Ne ring-laser gyroscopes [23,24]. Their simulations also showed that the additive quantum noise is involved in unlocking the system [24].

IV. EXPERIMENTS

The experiments were performed with the apparatus outlined in Fig. 5. The dye laser is in the form of a four-mirror folded ring laser, as described previously [26]. The active medium is a 2.3×10^{-4} molar solution of rhodamine B in water and methanol and is made to flow continuously through a 1-mm-thick dye cell. The dye laser is optically pumped by the 514.5-nm line of an argon-ion laser. Three uncoated étalons of thickness 0.1, 1, and 20 mm are inserted to ensure single-frequency operation. The wavelength of the dye laser is 603 nm during the measurements. The backscattering is provided by a 0.15-mm-thick uncoated intracavity glass plate G which is aligned perpendicular to the laser axis. During some of our measurements, the backscattering is controlled by changing the angular alignment of the thick étalon (20 mm) alone. The ring laser is operated very close to the symmetric configuration ($a_1=a_2$) by keeping the average intensities of the two counterpropagating modes nearly

equal.

The optical spectrum of the ring laser is monitored and measured by using two scanning Fabry-Pérot interferometers, with free spectral ranges of 2 GHz and 300 MHz and finesses of 50 and 300, respectively. The two output intensities of the laser are measured with two photodiodes each of 4 MHz bandwidth. The diode output signals are simultaneously recorded by two DSP Technology analog-to-digital converters (ADC's) that have 12-bit precision and 2 MHz bandwidth. A PDP/11-73 computer is used to read the time records of the intensities from the memory of the ADC unit through the CAMAC Dataway. For measuring intensity oscillations above 2 MHz, a pair of fast photodiodes with 100 MHz bandwidth is used in conjunction with a 300-MHz oscilloscope. A Spectra-Physics 401B power meter is used to calibrate the output signal from the photodiodes.

In our measurements, tuning the dye laser to the "off phase" backscattering condition is achieved in the following way. The laser is first adjusted to oscillate at a single frequency, by monitoring one of the output intensities with the two scanning Fabry-Pérot interferometers FP1,FP2. Then the pump power of the argon-ion laser is decreased until the dye laser is operating close to threshold. In this case the pump parameter is small and this results in a small value of R_c. The intracavity glass plate or the 2-mm étalon is then aligned to reflect the backscattered light onto the counterpropagating beams, and it is fine adjusted to produce stable intensity oscillations of maximum modulation. During the adjustment, the laser intensities are monitored by photodiodes and their values are continuously displayed on the oscilloscope. The backscattering coefficient $|R|$ is kept constant during each series of measurements. Instead of varying $|R|$ to change the laser from oscillations to switching, we vary R_c by changing the pump power of the argon-ion laser. An increase in the pump parameter of the dye laser results in an increase in the value of R_c. When R_c becomes larger than $|R|$, the dye laser changes from anticorrelated oscillations to random switching. Therefore, by adjustment of the pump power of the argon-ion laser, the intensities of dye laser can be tuned between oscillations and switching. With the laser operating in various stages, the two output intensities are recorded with the transient digitizer. In our experiments, it was not possible to fine tune $\delta\theta$ when the backscattering was due either to the intracavity glass plate or the 2-mm étalon. Moving either intracavity element in any direction along the laser axis does not change $\delta\theta$. Fine tuning of θ_1 and θ_2 can be achieved by using external mirrors that provide the backscattering [5,14].

Figure 6 shows the optical spectrum of one of the oscillating modes, as measured with a scanning Fabry-Pérot interferometer having a free spectral range of 300 MHz and resolution of 1 MHz. The spectrum shows a frequency splitting measured to be 16.7 MHz. The corresponding frequency of the intensity oscillations was determined to be 16.4 MHz with two 100-MHz-bandwidth photodiodes connected to a 300-MHz-bandwidth oscilloscope. The difference in the height of the two peaks is believed to be due to pump fluctuations and the slow scan rate of the Fabry-Pérot interferometer. Using the value $v=16.7$ MHz and the equation $|R|=\pi/T$, the value of $|R|$ in real units is determined to be 5.25×10^7 sec^{-1}. The amplitude reflectivity r is found to be 0.15 by using the formula $|R|=(cr)/L$, where c is the speed of light and L is the cavity length (0.84 m for our laser). The intensity reflectivity r^2 for this case is 2% and is reasonably close to what is expected for an uncoated optical surface. In the previous calculation, the equation $|R|=\pi/T$ has been used because $|R| \gg R_c$ and the frequency lock-in effect in

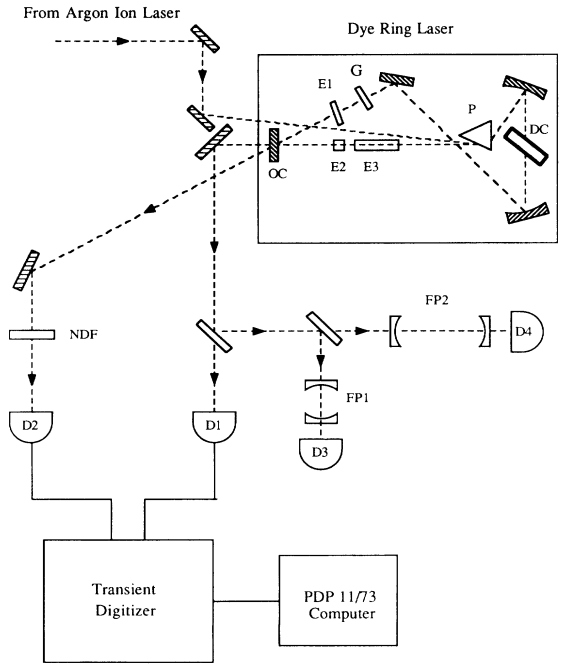

FIG. 5. A schematic diagram of the experimental setup. Inside the dye ring laser, E1, E2, and E3 are, respectively, 0.15-, 1-, and 20-mm uncoated étalons; G is the backscattering glass plate, DC is the dye cell; P is the intracavity prism; and OC is the output coupler. FP1 and FP2 are scanning Fabry-Pérot interferometers. D1–D4 are photodiodes. NDF is the neutral density filter.

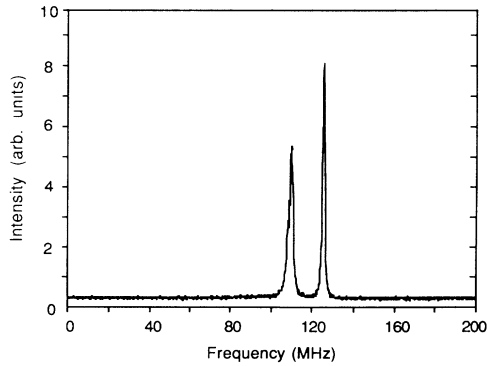

FIG. 6. Optical spectrum of one of the oscillating modes. The frequency splitting was determined to be 16.7 MHz and the frequency of the intensity oscillations was measured to be 16.4 MHz.

this region is negligible. Similar frequency splitting has been measured in a He-Ne laser [8] and in a dye ring laser [15].

Figure 7 shows the measured time evolution of the two intensities $I_1(t)$ and $I_2(t)$ recorded with an ADC sampling rate of 2 MHz. The intensity oscillations are anticorrelated and anharmonic. The period is approximately 9 μsec. The ratio of $|R|$ to R_c is found to be 1.2. This ratio is determined by keeping $|R|$ fixed and measuring the ratio of the intensities at which the laser change from oscillation to switching to the amplitude of these oscillations. This is justified because R_c is proportional to the pump parameter a, which in turn is proportional to the light intensity. Therefore, $|R|/R_c$ can be determined by measuring I_c/I, where I is the amplitude of the oscillations in Fig. 7 and I_c is the threshold intensity at which the laser changes from oscillations to switching. The small amplitude fluctuations are due to pump fluctuations as shown in the simulations. The measured data show that neither of the two intensities vanishes during the oscillations, which indicates a small but nonzero $\delta\theta$. Figure 7 can be compared with the simulation results shown in Fig. 2 in which $|R|/R_c$ is also equal to 1.2. In our experiments, the intensity oscillations are found to become nearly harmonic when the ratio $|R|/R_c$ becomes large. Harmonic oscillation was also observed by Schroter and Kuhlke [14] and by Cresser *et al.* [23].

We have observed a frequency lock-in effect when the intensities of the dye laser is tuned from anticorrelated oscillations to random switching. For a fixed $|R|$, the frequency of the oscillations is found to decrease with increasing pump power of the argon-ion laser. We attribute this effect to lock-in of the two optical frequencies of the standing-wave mode. Figure 8 shows a plot of the oscillation frequency of the intensities versus the pump parameter. Instead of studying the oscillation frequency as a function of $|R|$, we measured the frequency of the intensity oscillations as a function of the amplitude of the oscillations, which corresponds to the pump parameter. This is because $|R|$ cannot be varied systematically with our current experimental setup. The data shown are measurements for three different values of $|R|$. The solid

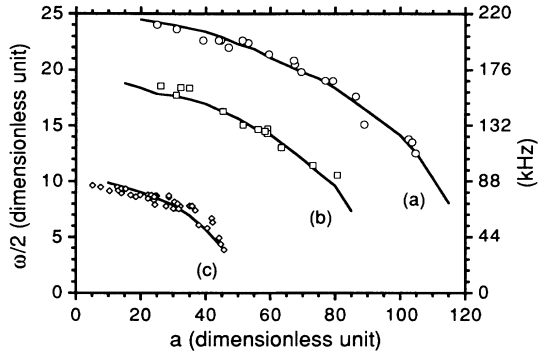

FIG. 8. Plot of intensity oscillation frequency vs pump parameter. The values of $|R|$ for curves (a), (b), and (c) are 6.9×10^5 sec^{-1}, 5.3×10^5 sec^{-1}, and 2.8×10^5 sec^{-1}, respectively. The solid curves are simulation results for $|R|=25$, 19, and 10 in dimensionless units.

curves are obtained from Monte Carlo simulations on Eqs. (1)–(6), with the multiplicative-noise terms neglected. Each curve is formed by joining more than 20 computed points together. Each point is obtained by averaging over two simulations. The roughness of the curves is due to the additive noise and can be removed by averaging over more realizations from the simulations. All data in Fig. 8 are fitted with a single scale factor such that one dimensionless unit of time corresponds to 3.6×10^{-5} sec. The values of $|R|$ in real units for the three curves are determined to be 6.9×10^5 sec^{-1}, 5.3×10^5 sec^{-1}, and 2.8×10^5 sec^{-1}, and are independent of the scale factor. The corresponding values in dimensionless units are 25, 19, and 10.

Figure 9 shows the two recorded intensities $I_1(t)$ and $I_2(t)$ when the value of $|R|$ was very close to R_c. As the figure indicates, when the intensity is larger than a certain value, the laser exhibits mode switching, while below this value, it exhibits periodic oscillations. This is similar to the simulations shown in Fig. 3 and has been explained above as due to the effect of pump fluctuations. By measuring the oscillation intensities for various pump parameters and plotting a similar diagram, such as Fig. 8, we determine $|R|$ to be 5.8×10^5 sec^{-1} in real units. The

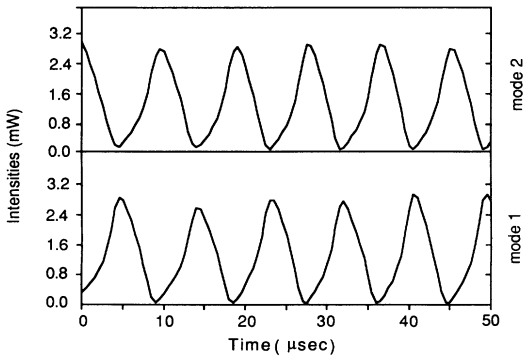

FIG. 7. Plots of the measured intensities vs time when $|R|/R_c=1.2$. The intensity oscillations are anharmonic.

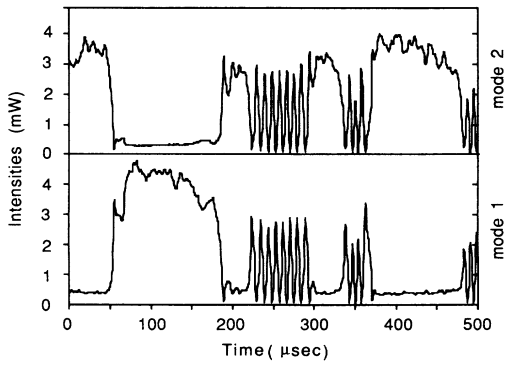

FIG. 9. Time records of measured intensities of the dye ring laser when $|R|$ is close to R_c. Due to the effect of pump fluctuations, the laser exhibits both switching and oscillations.

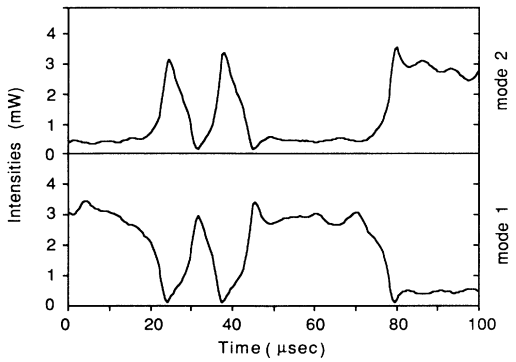

FIG. 10. Time evolution of measured intensities similar to Fig. 9 but with an expanded time scale. The ratio of the two switching intensities is approximately equal to 8 and is close to the theoretically predicted value 7.9.

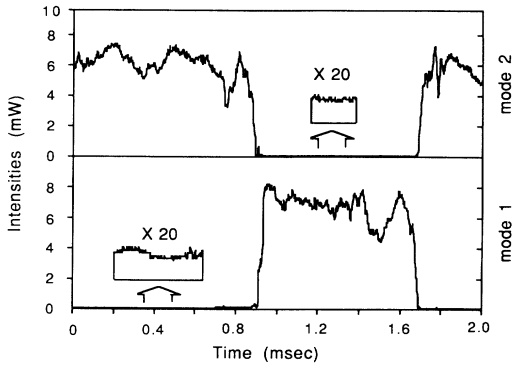

FIG. 11. Time evolution of the measured intensities when the laser is operated in the switching region. Insets show the intensities of the "off" mode with a vertical magnification of 20. The ratio of the average "on" intensity to the average "off" intensity is about 100.

corresponding value in dimensionless units is 21. From Eq. (9), the value of the pump parameter of the dye laser at $|R|=R_c$ is determined to be 2.8×10^6 sec^{-1} in real units. This value lies within the range of pump parameters for another dye laser operated not far above threshold determined by Roy, Yu, and Zhu [27]. Figure 10 shows records of the two measured intensities near $|R|=R_c$ on an expanded time scale. The period of the oscillations is measured to be 13.3 μsec. The oscillations are anharmonic and are consistent with the predictions of both the deterministic analysis and the Monte Carlo simulations. In the switching region, the ratio of the two intensities at $|R|=R_c$ is found to be approximately equal to 8, which is close to the theoretical value of 7.9 obtained from Eq. (10).

Figure 11 shows records of the two mode intensities when the laser is operated in the switching region. The insets show the intensities of the "off" mode with a vertical magnification of 20. The most probable intensity of the "off" mode is nonzero and this is different from the case without backscattering. The ratio of the intensity of the "on" mode to the "off" mode is found to increase with increasing pump parameter, and this is consistent with both our simulation results and the deterministic analysis [2]. In Fig. 11, the ratio of the "on" intensity to the "off" intensity is measured to be about 100. By measuring the oscillation intensities with various pump parameters and plotting a diagram such as Fig. 8, we determine $|R|$ to be 2.4×10^5 sec^{-1}. The ratio $a/|R|$ is approximately 20. Using the formula obtained from the deterministic analysis [2] for $\delta\theta=0$, the value of the intensity ratio is calculated to be 390. From Monte Carlo simulations, the intensity ratio obtained for $a/|R|=20$ and $\delta\theta$ equal to 10° is 389. The large discrepancy between the measured intensity ratio and the calculated value is not well understood. Other measurements show that the discrepancy becomes smaller when the pump parameter is decreased. When $R_c=|R|$, where $a/|R|=4.9$, the measured value is consistent with the theoretical prediction. The discrepancy may be related to the accuracy of measuring the small intensities of the "off" mode. It may also be connected with the use of the third-order laser theory for the calculations and simulations, even when the laser operates far above threshold.

V. CONCLUSION

The dynamics of the two intensities of the dye ring laser with near "off phase" backscattering have been investigated experimentally. We have observed the two counterpropagating intensities of the dye ring laser change from random switching to anticorrelated oscillations by varying the pump power of the argon-ion laser. Noise-induced transitions between the switching region and the oscillation region are experimentally observed when $|R|$ is close to R_c. We attribute this noise-induced effect to the pump fluctuations whose large fluctuating strength dominates over the effect of the spontaneous emission noise. The ratio of the "on" intensity to the "off" intensity at $|R|=R_c$ is determined to be 8 and is consistent with the theoretically predicted value of 7.9. When the laser is operated in the oscillation region, the period of the oscillations is found to change with the pump parameter. This can be attributed to the lock-in effect of the two standing-wave mode frequencies. The experimental results are compared with the analytic solution of the deterministic equations of motion and with the Monte Carlo simulation results. All experimental results are found to be in good agreement with the theory, except for the ratio of the "on" intensity to the "off" intensity when the laser is operated well inside the switching region with $|R| \ll R_c$.

ACKNOWLEDGMENTS

The author is very grateful to Dr. L. Mandel for his advice and support. This research was supported by the National Science Foundation and by the U.S. Office of Naval Research.

[1] W. W. Chow, J. Gea-Banacloche, L. M. Pedrotti, V. E. Sanders, W. Schleich, and M. O. Scully, Rev. Mod. Phys. **57**, 61 (1985).
[2] D. Kuhlke and G. Jetschke, Physica C **106**, 287 (1981).
[3] D. Kuhlke, Acta Phys. Pol. A **61**, 547 (1982).
[4] W. R. Christian, T. H. Chyba, E. C. Gage, and L. Mandel, Opt. Commun. **66**, 238 (1988).
[5] T. H. Chyba, Phys. Rev. A **40**, 6327 (1989).
[6] T. H. Chyba, Opt. Commun. **76**, 395 (1990).
[7] T. H. Chyba, Proc. SPIE **1376**, 132 (1991).
[8] R. J. C. Spreeuw, R. Centeno Neelen, N. J. van Druten, E. R. Eliel, and J. P. Woerdman, Phys. Rev. A **42**, 4315 (1990).
[9] L. Pesquera, R. Blanco, and M. A. Rodriguez, Phys. Rev. A **39**, 5777 (1989); L. Pesquera and R. Blanco, Opt. Commun. **74**, 102 (1989).
[10] W. R. Christian and L. Mandel, Phys. Rev. A **34**, 3932 (1986); **36**, 1510 (1987).
[11] W. R. Christian and L. Mandel, J. Opt. Soc. Am. B **5**, 1406 (1988).
[12] D. Kuhlke and R. Horak, Physica C **111**, 111 (1981).
[13] R. Roy and L. Mandel, Opt. Commun. **35**, 247 (1980).
[14] S. Schroter and D. Kuhlke, Opt. Quantum Electron **13**, 247 (1981).
[15] R. Centeno Neelen, R. J. C. Spreeuw, E. R. Eliel, and J. P. Woerdman, J. Opt. Soc. Am. B **8**, 959 (1991).
[16] F. C. Cheng, Opt. Commun. **82**, 45 (1991).
[17] S. Singh and L. Mandel, Phys. Rev. A **20**, 2459 (1979).
[18] R. Roy and L. Mandel, Opt. Commun. **34**, 133 (1980).
[19] P. Lett, W. Christian, S. Singh, and L. Mandel, Phys. Rev. Lett. **47**, 1892 (1981).
[20] P. Lett and L. Mandel, J. Opt. Soc. Am. B **2** 1615 (1985).
[21] E. C. Gage and L. Mandel, Phys. Rev. A **38**, 5166 (1981).
[22] E. C. Gage and L. Mandel, J. Soc. Opt. Am. B **6**, 287 (1989).
[23] J. D. Cresser, W. H. Louisell, P. Meystre, W. Schleich, and M. O. Scully, Phys. Rev. A **25**, 2214 (1982).
[24] J. D. Cresser, D. Hammonds, W. H. Louisell, P. Meystre, and H. Risken, Phys. Rev. A **25**, 2226 (1982).
[25] W. E. Lamb, Jr., Phys. Rev. **134**, A 1429 (1964).
[26] F. C. Cheng and L. Mandel, J. Opt. Soc. Am. B **8**, 1681 (1991).
[27] R. Roy, A. W. Yu, and S. Zhu, Phys. Rev. Lett. **55**, 2794 (1985); Phys. Rev. A **34**, 4333 (1990).

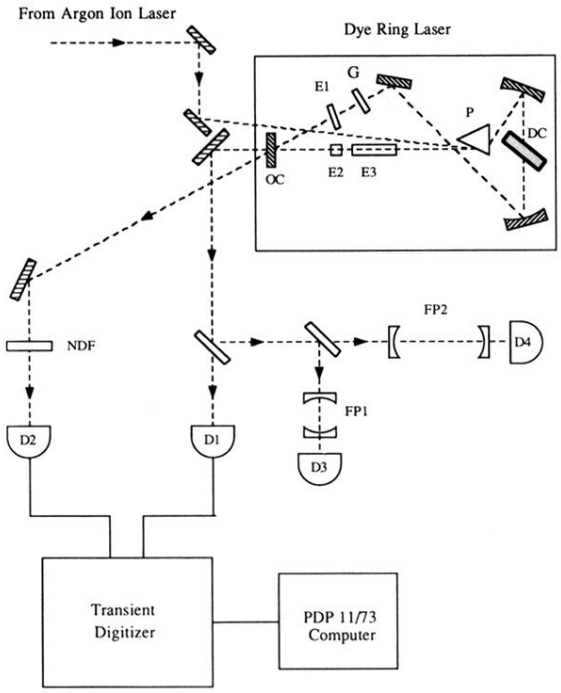

FIG. 5. A schematic diagram of the experimental setup. Inside the dye ring laser, E1, E2, and E3 are, respectively, 0.15-, 1-, and 20-mm uncoated étalons; G is the backscattering glass plate, DC is the dye cell; P is the intracavity prism; and OC is the output coupler. FP1 and FP2 are scanning Fabry-Pérot interferometers. D1–D4 are photodiodes. NDF is the neutral density filter.